ACOUSTICS 2012

# Recovery of the free field using the spherical wave superposition method

C.-X. Bi, D.-Y. Hu, L. Xu and Y.-B. Zhang

Institute of Sound and Vibration Research, Hefei University of Technology, 230009 Hefei, China
cxbi@hfut.edu.cn

As a preprocessing technique of nearfield acoustic holography, sound field separation technique could separate the non-free field into two parts: the outgoing field and the incoming field. Generally, the former is used for sound source reconstruction. In fact, the outgoing field consists of the field radiated by the source in a free-field and the field scattered on the source surface caused by the incoming field. When the scattered field could not be neglected, the reconstruction using the outgoing field would be erroneous. To separate the radiated field and scattered field, a free-field recovery technique using the spherical wave superposition method is proposed. A theoretical description is first given, and then two numerical simulations are used to demonstrate the validity of this technique.

# 1 Introduction

Near-field acoustic holography (NAH) [1,2] has been proved to be a powerful tool for sound field visualization and reconstruction since it was first proposed in 1980s. The conventional NAH requires the sound field is free, that is to say, the sound field just contains the outgoing wave radiated by the target source. However, in practice the sound field is often disturbed by the incoming wave due to the reflection or the disturbing source. In order to reduce or remove the disturbance from the incoming wave, two methods can be used. One is to carry out the measurement in the very near field of the target source to get high signal-to-noise ratio (SNR) signals, and combine with the use of regularization method to reduce the influence of the incoming wave in the reconstruction process. This method is especially effective when the particle velocity is used to reconstruct the sound field [3]. The other is to remove the incoming wave using sound field separation technique (SFST). Several different SFSTs have been developed for this purpose [4-8]. Moreover, in practice the outgoing wave contains not only the wave radiated by the target source in the free field, but also the wave scattered on the target source surface caused by the incoming wave. When the scattering effect could not be neglected, the reconstruction using the outgoing field would be erroneous. To remove the scattered field from the outgoing field, a separation method based on boundary element method was proposed by Langrenne *et al.* [9,10]. Hald *et al.* [11] also realized this separation by using sound intensity method based on statistically optimized nearfield acoustic holography. Recently, the equivalent source method is used for the same purpose by Bi and Bolton. [12]. In this paper, an alternative method based on the spherical wave superposition is utilized to realize this separation.

# 2 Theoretical background

## 2.1 Spherical wave superposition method

For the exterior problems, the sound field can be presented by a series of spherical harmonics expansion. The sound pressure at any point in the spherical coordinate system can be approximated by

$$p(r,\theta,\phi) \approx \sum_{n=0}^{N}\sum_{m=-n}^{n} C_{mn} h_n(kr) Y_n^m(\theta,\phi) = \sum_{j=0}^{J} C_j \psi_j(r,\theta,\phi,\omega), \quad (1)$$

where $Y_n^m(\theta,\phi)$ is spherical harmonics function, $j = n^2 + n + m + 1$, $J = (N+1)^2$, $h_n(kr)$ is Hankel function of the first kind, and $N$ is the cutoff order of spherical harmonics.

Eq. (1) can be written in a matrix form as

$$\mathbf{p} = \mathbf{\Psi C}, \quad (2)$$

where

$$\mathbf{p} = [p_{r1}\ p_{r2} \cdots p_{rM}]^T, \quad (3)$$

$$\mathbf{C}(\omega) = [C_1\ C_2 \cdots C_J)]^T, \quad (4)$$

$$\mathbf{\Psi}(\omega) = \begin{bmatrix} \psi_1(r_1) & \psi_2(r_1) & \cdots & \psi_J(r_1) \\ \psi_1(r_2) & \psi_2(r_2) & \cdots & \psi_J(r_2) \\ \vdots & \vdots & \ddots & \vdots \\ \psi_1(r_M) & \psi_2(r_M) & \cdots & \psi_J(r_M) \end{bmatrix}, \quad (5)$$

where $\mathbf{p}$ is sound pressure column vector on any measurement surface, the superscript "$T$"' denotes the matrix transpose, $r_i$ represent the $i$th measurement point, $M$ is the number of measurement points, $\mathbf{\Psi}$ is the spherical wave source matrix of pressure, and $\mathbf{C}$ is the weight coefficient column vector.

For the interior problems, $h_n(kr)$ in the above equations needs to be replaced by $j_n(kr)$.

## 2.2 Separation of incoming field and outgoing field

When the disturbing source exists, the sound field can be separated into the incoming field and the outgoing field. The sound pressure on any measurement surface can be expressed as

$$\mathbf{p} = \mathbf{p}_{out} + \mathbf{p}_{in}, \quad (6)$$

where

$$\mathbf{p}_{out} = \mathbf{\Psi}_p^{out} \mathbf{C}_{out}, \quad (7)$$

$$\mathbf{p}_{in} = \mathbf{\Psi}_p^{in} \mathbf{C}_{in}. \quad (8)$$

In Eqs. (6)-(8), the quantities with the symbols "*in*", "*out*" and the subscript "*p*" imply that they are related to the incoming field, the outgoing field and the pressure, respectively, $\mathbf{\Psi}_p^{out}$ is the outgoing spherical wave source matrix of pressure constructed by $h_n(kr)Y_n^m(\theta,\phi)$, and $\mathbf{\Psi}_p^{in}$

is the incoming spherical wave source matrix of pressure constructed by $j_n(kr)Y_n^m(\theta,\phi)$.

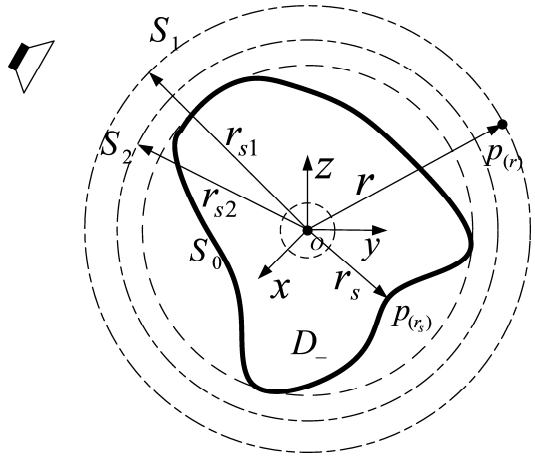


Figure 1: Separation diagram: the spherical wave sources are located at the center of the least circumscribed sphere of sound source. $S_0$ is the target source surface. The measurement surfaces are two closely spaced spherical surfaces $S_1$ and $S_2$.

To solve the outgoing weight coefficient column vector $\mathbf{C}_{out}$ and the incoming weight coefficient column vector $\mathbf{C}_{in}$, the measurements need to be performed on two surfaces $S_1$ and $S_2$ as shown in Fig. 1. Then the measured two sound pressure column vectors $\mathbf{p}_1$ and $\mathbf{p}_2$ are combined into one vector and expressed by using Eqs. (6)-(8) as

$$\begin{bmatrix}\mathbf{p}_1\\ \mathbf{p}_2\end{bmatrix}=\begin{bmatrix}\boldsymbol{\Psi}_p^{out,1} & \boldsymbol{\Psi}_p^{in,1}\\ \boldsymbol{\Psi}_p^{out,2} & \boldsymbol{\Psi}_p^{in,2}\end{bmatrix}\begin{bmatrix}\mathbf{C}_{out}\\ \mathbf{C}_{in}\end{bmatrix}, \tag{9}$$

where the numbers "1" and "2" denote the measurement surface $S_1$ and the measurement surface $S_2$, respectively. Finally the weight coefficient column vectors $\mathbf{C}_{out}$ and $\mathbf{C}_{in}$, can be solved by the inversion of Eq. (9) as

$$\begin{bmatrix}\mathbf{C}_{out}\\ \mathbf{C}_{in}\end{bmatrix}=\begin{bmatrix}\boldsymbol{\Psi}_p^{out,1} & \boldsymbol{\Psi}_p^{in,1}\\ \boldsymbol{\Psi}_p^{out,2} & \boldsymbol{\Psi}_p^{in,2})\end{bmatrix}^{+}\begin{bmatrix}\mathbf{p}_1\\ \mathbf{p}_2\end{bmatrix}. \tag{10}$$

Once $\mathbf{C}_{out}$ and $\mathbf{C}_{in}$ are obtained, the outgoing pressure on the measurement surface $S_1$, can be calculated by

$$\mathbf{p}_{1,out}=\boldsymbol{\Psi}_p^{out,1}\mathbf{C}_{out}, \tag{11}$$

and the incoming pressure and normal velocity on the source surface $S_0$ can be also calculated by

$$\mathbf{p}_{0,in}=\boldsymbol{\Psi}_p^{in,0}\mathbf{C}_{in}, \tag{12}$$

$$\mathbf{v}_{0,in}=\boldsymbol{\Psi}_v^{in,0}\mathbf{C}_{in}, \tag{13}$$

where the symbol "0" denotes the source surface, and $\boldsymbol{\Psi}_p^{in,0}$ and $\boldsymbol{\Psi}_v^{in,0}$ are the incoming spherical wave source matrices of pressure and particle velocity, respectively.

## 2.3 Separation of radiated field and scattered field

On the target source surface $S_0$, when the scattering caused by the incoming waves exists, the relationship between sound pressure and normal particle velocity can be represented by

$$\mathbf{v}_{0,in}+\mathbf{v}_{0,scat}=\mathbf{Y}_0(\mathbf{p}_{0,in}+\mathbf{p}_{0,scat}). \tag{14}$$

In Eq. (14), the symbol "*scat*" denotes the scattered field, $\mathbf{Y}_0$ is admittance matrix of the target source surface, $\mathbf{p}_{0,in}$ and $\mathbf{v}_{0,in}$ can be calculated by using Eqs. (12) and (13), and the scattered pressure and normal velocity $\mathbf{p}_{0,scat}$ and $\mathbf{v}_{0,scat}$ is expressed, respectively, as

$$\mathbf{v}_{0,scat}=\boldsymbol{\Psi}_v^{scat,0}\mathbf{C}_{scat}, \tag{15}$$

$$\mathbf{p}_{0,scat}=\boldsymbol{\Psi}_p^{scat,0}\mathbf{C}_{scat}, \tag{16}$$

where $\mathbf{C}_{scat}$ is the weight coefficient column vector of scattered field, and $\boldsymbol{\Psi}_p^{scat,0}$ and $\boldsymbol{\Psi}_v^{scat,0}$ are the scattering spherical wave source matrices of pressure and particle velocity, respectively. Generally, $\boldsymbol{\Psi}_p^{scat,0}$ and $\boldsymbol{\Psi}_v^{scat,0}$ can be replaced by $\boldsymbol{\Psi}_p^{out,0}$ and $\boldsymbol{\Psi}_v^{out,0}$, respectively.

Substituting Eqs. (15) and (16) into Eq. (14), and replacing $\boldsymbol{\Psi}_p^{scat,0}$ and $\boldsymbol{\Psi}_v^{scat,0}$ with $\boldsymbol{\Psi}_p^{out,0}$ and $\boldsymbol{\Psi}_v^{out,0}$ respectively, yields

$$\mathbf{v}_{0,in}-\mathbf{Y}_0\mathbf{p}_{0,in}=(-\boldsymbol{\Psi}_v^{out,0}+\mathbf{Y}_0\boldsymbol{\Psi}_p^{out,0})\mathbf{C}_{scat}. \tag{17}$$

By the inversion of Eq. (17), the weight coefficient column vector of scattered field $\mathbf{C}_{scat}$ can be obtained as

$$\mathbf{C}_{scat}=(-\boldsymbol{\Psi}_v^{out,0}+\mathbf{Y}_0\boldsymbol{\Psi}_p^{out,0})^{+}(\mathbf{v}_{0,in}-\mathbf{Y}_0\mathbf{p}_{0,in}). \tag{18}$$

Note that when the target source surface $S_0$ is rigid, that is the admittance matrix of the target source surface $\mathbf{Y}_0$ is a zero matrix, Eq. (18) can be simplified into

$$\mathbf{C}_{scat}=-(\boldsymbol{\Psi}_v^{out,0})^{+}\mathbf{v}_{0,in}. \tag{19}$$

Once $\mathbf{C}_{scat}$ is obtained, the scattered pressure on the measurement surface $S_1$ can be calculated by

$$\mathbf{p}_{1,scat}=\boldsymbol{\Psi}_p^{out,1}\mathbf{C}_{scat}. \tag{20}$$

Finally, the free-field pressure $\mathbf{p}_{1,rad}$ radiated by the target source on the measurement surface $S_1$ is recovered by

subtracting the scattered pressure $\mathbf{p}_{1,scat}$ from the outgoing pressure $\mathbf{p}_{1,out}$ as

$$\mathbf{p}_{1,rad} = \mathbf{p}_{1,out} - \mathbf{p}_{1,scat} . \quad (21)$$

If the recovered free-field pressure $\mathbf{p}_{1,rad}$ is then used to reconstruct the field radiated by the target source, the whole free-field can be recovered.

# 3 Numerical Simulations

Simulations are carried out to investigate the validity of the free-field recovery technique based on the spherical wave superposition method. A rigid sphere with an upper sphere cap is used as the target source. The radius of sphere is $a = 0.5$ m , the sphere cap is defined by an angle of $\alpha = \pi/10$ radians and vibrated with a velocity amplitude of $v = 1$ m/s . Two cases are investigated when the rigid sphere is located near a point source and located in a concentric spherical cavity, respectively. In these two cases, sound pressures are measured on two spherical surfaces with the radii of $r_1$ = 0.6 m and $r_2$ = 0.57 m. A Gauss white noise with the SNR of 40 dB is added into the measured data.

## 3.1 Spherical wave scattering by a rigid sphere with a vibrating spherical cap

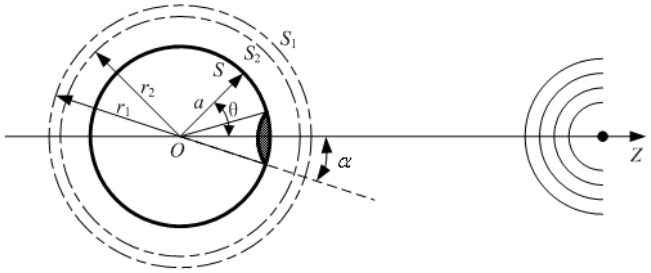


Figure 2: Geometry of case 1: the rigid sphere is located near a point source. $S$ is the target source surface. $S_1$ and $S_2$ are the two measurement surfaces.

As shown in Fig. 2, the point source is located at (0, 0, 2m), and its radiating sound power is chosen to equal that of the sphere cap. Here, the radiating sound power on any surface $\Omega$ is defined as

$$POW = \int_{\Omega} \frac{|p(\mathbf{r})|^2}{\rho_0 c} d\Omega , \quad (22)$$

where $p(\mathbf{r})$ is the sound pressure at any point $\mathbf{r}$ on the surface $\Omega$ .

Because of the symmetry of the sound field around the z-axis on the measurement surface $S_1$, only the sound pressure along $\theta$ -direction is calculated. Figure 3 shows the real and imaginary parts of the outgoing pressure, the recovered free-field pressure radiated by the target source using the spherical wave superposition method and the theoretical free-field pressure radiated by the target source for $ka$ = 3.6. It can be found that owing to the effect of the scattered pressure, the outgoing pressure is different from the theoretical free-field pressure radiated by the target source. By applying the proposed free-field recovery technique to remove the scattered pressure, the recovered free-field pressure radiated by the target source shows good agreement with its theoretical value.

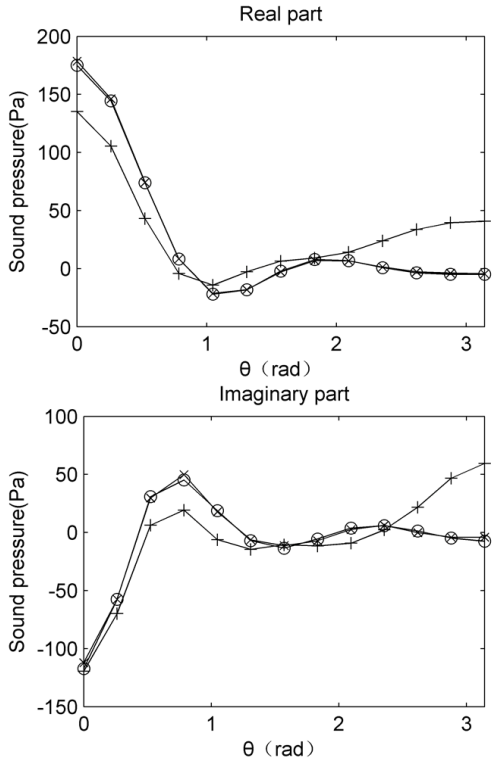


Figure 3: The real and imaginary parts of the theoretical free-field pressure radiated by the target source (“o”), the recovered free-field pressure radiated by the target source using the spherical wave superposition method (“×”) and the outgoing pressure (“+”) on the measurement surface $S_1$ when $ka$ = 3.6.

To quantitatively describe the difference, the relative error is defined by

$$\zeta = \frac{\left\| \tilde{\mathbf{p}} - \hat{\mathbf{p}} \right\|_2}{\left\| \hat{\mathbf{p}} \right\|_2} \times 100\% , \quad (23)$$

where $\| \bullet \|_2$ denotes the matrix 2-norm, $\hat{\mathbf{p}}$ represents the theoretical free-field pressure radiated by the target source, and $\tilde{\mathbf{p}}$ is the outgoing pressure or the recovered free-field pressure.

The relative errors corresponding to different $ka$ are calculated by Eq. (23). Figure 4 shows that the relative errors between the theoretical free-field pressure and the outgoing pressure increase with $ka$, while the relative errors between the theoretical free-field pressure and the recovered free-field pressure remain below 10%. This is because the amplitude of the scattered pressure included in the outgoing pressure increases with $ka$. In particular, when $ka$ is large, the scattered pressure has to be removed from the outgoing pressure to guarantee the validity of the reconstruction.

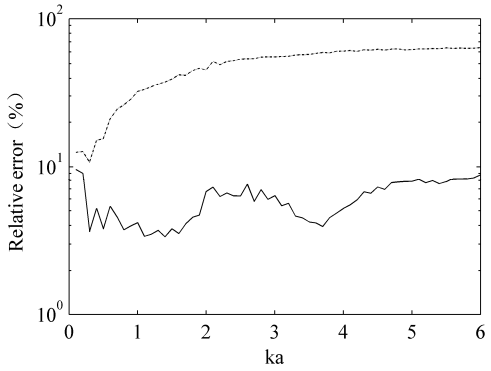


Figure 4: The relative errors between the theoretical free-field pressure and the outgoing pressure (dotted line), and those between the theoretical free-field pressure and the recovered free-field pressure (solid line).

## 3.2 A rigid sphere with a vibrating spherical cap inside a rigid spherical cavity

As shown in Fig. 5, the rigid sphere is placed in a concentric spherical cavity with a radius of $b$ = 1.25m. The incoming wave is from the reflection of the wall of the cavity.

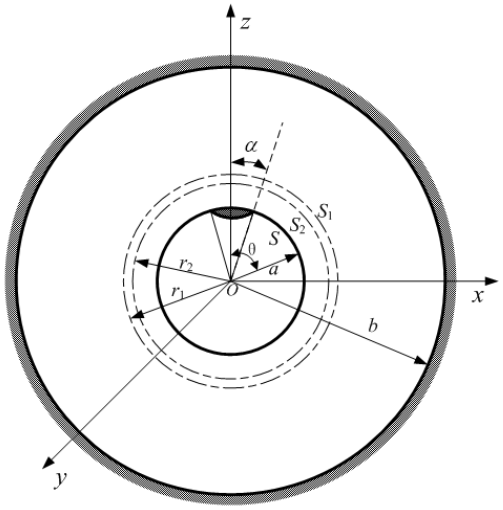


Figure 5: Geometry of case 2. The rigid sphere is located inside a concentric spherical cavity. $S$ is the surface of the source. $S_1$ and $S_2$ are the two separation surfaces.

Similarly, only the sound pressure along θ -direction on the measurement surface $S_1$ is calculated. Figure 6 gives the real and imaginary parts of the outgoing pressure, the separated free-field pressure radiated by the target source using the spherical wave superposition method and the theoretical free-field pressure radiated by the target source for $ka$ = 4.5. From Fig. 6, it is seen that the outgoing pressure is very different from the theoretical free-field pressure radiated by the target source, and the proposed free-field recovery technique can effectively remove the scattered pressure from the outgoing pressure.

Figure 7 shows that the relative errors between the theoretical free-field pressure and the outgoing pressure, and those between the theoretical free-field pressure and the recovered free-field pressure corresponding to different $ka$. It can be found that the relative errors between the theoretical free-field pressure and the outgoing pressure are clearly larger than those between the theoretical free-field pressure and the recovered free-field pressure, which further demonstrates the necessity the proposed free-field recovery technique. In addition, oscillations appear in both relative error curves. This is probably caused by the modal behaviour of the cavity, which is proved by comparing the relative error curves with the sound power level curve on the measurement surface $S_1$ as shown in Fig. 8. At the modal frequencies, the scattered pressure is dramatically large while the radiated pressure is very small, so the radiated pressure is badly contaminated by the scattered pressure, which leads to the larger relative errors at the modal frequencies.

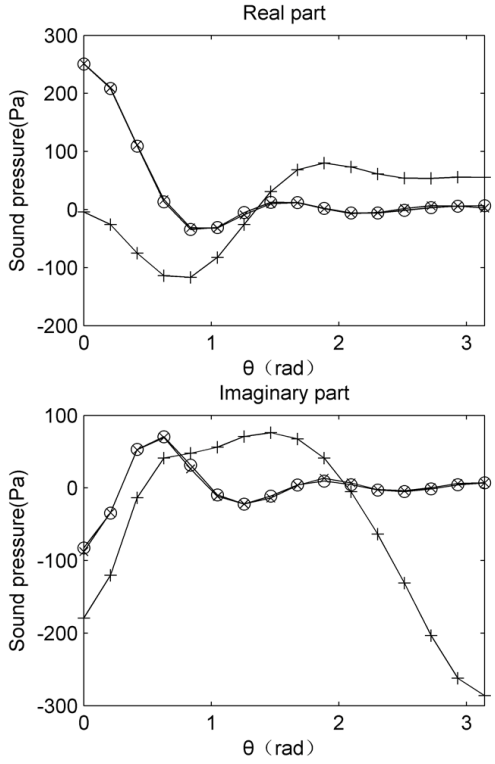


Figure 6: The real and imaginary parts of the theoretical free-field pressure radiated by the target source (“o”), the recovered free-field pressure radiated by the target source using the spherical wave superposition method (“×”) and the outgoing pressure (“+”) on the measurement surface $S_1$ when $ka$ = 4.5.

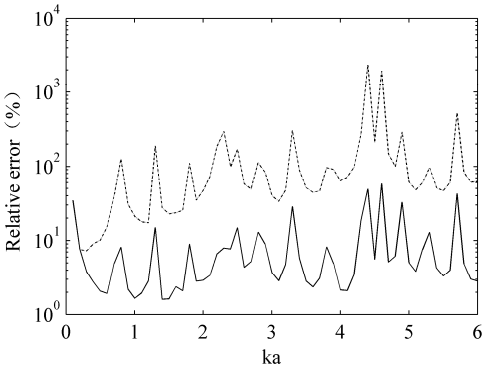


Figure 7: The relative errors between the theoretical free-field pressure and the outgoing pressure (dotted line), and those between the theoretical free-field pressure and the recovered free-field pressure (solid line).

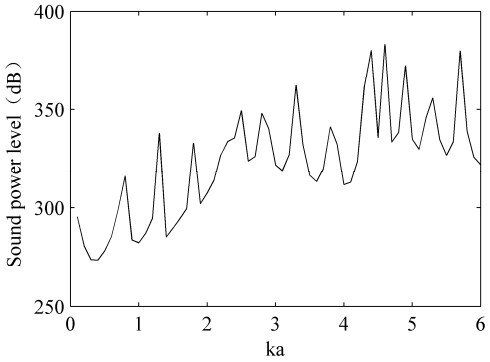


Figure 8: Sound power level on the surface $S_1$.

# 4 Conclusion

A free-field recovery technique based on the spherical wave superposition method was proposed. It not only can separate the outgoing field and the incoming field when the incoming wave due to the reflection or the disturbing source exists, but also can separate the field scattered on the target source surface caused by the incoming wave from the outgoing field. Two simulation cases demonstrated the validity and necessity of the proposed free-field recovery technique. However, an existing obstacle to use this technique is the measurement of the surface impedance. For most of machinery equipments, an approximate rigid boundary can be used; while for some elastic material, the impedance measurement methods are mostly for "locally reacting" surface, and the method for "extensively reacting" surface is too time-consuming and impractical. Therefore, it is a key issue to find an efficient method for measuring the impedance for "extensively reacting" surface.

# Acknowledgments

This work was supported by National Natural Science Foundation of China (Grant Nos. 10974040 and 11004045), the Program for New Century Excellent Talents in University (Grant No. NCET-08-0767), and the Research Fund for the Doctoral Program of Higher Education (Grand No. 20100111110007).

# References

[1] E. G. Williams, J. D. Maynard, E. Skudrzyk, "Sound source reconstruction using a microphone array", *J. Acoust. Soc. Am*. 68(1), 340-344 (1980)

[2] J. D. Maynard, E. G. Williams, Y. Lee, "Nearfield acoustic Holography I: Theory of generalized holography and the development of NAH", *J. Acoust. Soc. Am*. 78(4), 1395-1413 (1985)

[3] A. Vecchio, L. Valent, A. Berthe, H.-E. Debree, "The Microflown, a Novel Approach to Helicopters Interior Noise Testing", in *IMTC 2006*, Sorrento, Italy, 584-589 (2006)

[4] G. Weinreich, E. B. Arnold, "Method for measuring acoustic radiation fields", *J. Acoust. Soc. Am.* 68(2), 404-411 (1980)

[5] D. L. Hallman, J. S. Bolton, "A technique for performing source identification in reflective environments by using nearfield acoustical holography", in *Proceedings of Noise-Con 93*, Williamsburg, Virginia, 479-484 (1993)

[6] J. Hald, "Patch holography in cabin environments using a two-layer handheld array with an extended SONAH", in *Proceedings of Euronoise 2006*, Tampere, Finland (2006)

[7] F. Jacobsen, V. Jaud, "Statistically optimized near field acoustic holography using an array of pressure-velocity probes", *J. Acoust. Soc. Am*. 121(3), 1550-1558 (2007)

[8] C. X. Bi, X. Z. Chen, J. Chen, "Sound field separation technique based on equivalent source method and its application in nearfield acoustic holography", *J. Acoust. Soc. Am*. 123(3), 1472-1478 (2008)

[9] C. Langrenne, M. Melon, A. Garcia, "Boundary element method for the acoustic characterization of a machine in bounded noisy environment", *J. Acoust. Soc. Am*. 121(5), 2750-2757 (2007)

[10] C. Langrenne, M. Melon, A. Garcia, "Measurement of confined acoustic sources using near-field acoustic holography", *J. Acoust. Soc. Am*. 126(3), 1250-1256 (2009)

[11] J. Hald, J. Mørkholt, P. Hardy, D. Trentin, M. Bach-Andersen, G. Keith, "Array based measurement of radiated and absorbed sound intensity components", in *Proceedings of Euronoise 2008*, Paris, France, 2899-2904 (2008)

[12] C. X. Bi, J. Stuart Bolton, "An equivalent source technique for recovering the free sound field in a noisy environment", *J. Acoust. Soc. Am.* 131(2), 1260-1270 (2012)